Endothelial features along the pulmonary vascular tree in chronic thromboembolic pulmonary hypertension: distinctive or shared facets?

Janne Verhaegen[1*], Lynn Willems[1*], Allard Wagenaar[1], Ruben Spreuwers[1], Nessrine Dahdah[1], Lucia Aversa[1], Tom Verbelen[2,3], Marion Delcroix[1,4], Rozenn Quarck[1,4§]

Affiliations:

[1]Laboratory of Respiratory Diseases & Thoracic Surgery (BREATHE), Department of Chronic Diseases & Metabolism (CHROMETA), KU Leuven – University of Leuven, Leuven, Belgium

[2]Department of Cardiac Surgery, University Hospitals Leuven, Leuven, Belgium

[3]Department of Cardiovascular Sciences, KU Leuven - University of Leuven, Leuven, Belgium.

[4]Clinical Department of Respiratory Diseases, University Hospitals, Leuven, Belgium

**Equal contribution*

Running title: Endothelial features in CTEPH

§Corresponding author: Rozenn QUARCK, Laboratory of Respiratory Diseases & Thoracic Surgery (BREATHE), Department of Chronic Diseases & Metabolism (CHROMETA), KU Leuven, Herestraat 49, B-3000 Leuven, Belgium; Tel: +32 16 33 01 89; email: rozenn.quarck@kuleuven.be

Number of pages: 20
Number of figures: 8
Word count: 3429

Article type: original research article

Keywords: Chronic Thromboembolic Pulmonary Hypertension; Endothelial cells; Angiogenesis; Barrier function; Vascular remodelling

ABSTRACT

Background. Chronic thromboembolic pulmonary hypertension (CTEPH) is a rare complication of pulmonary embolism, characterised by organized fibro-thrombotic material that partially or fully obstructs large pulmonary arteries, microvasculopathy and enlargement of the bronchial systemic vessels. Although the underlying mechanisms of CTEPH remain unclear, deficient angiogenesis and altered pulmonary arterial endothelial cell (PAEC) function may contribute to disease progression. Although differences in histological features, shear stress and ischemia are observed along the pulmonary vascular tree, the potential contribution of PAEC phenotype and function to these different aspects remains unexplored. We consequently hypothesized that angiogenic capacities and endothelial barrier function could contribute to disparities of histological features observed along the pulmonary vascular tree.

Methods. We therefore explored histological aspects of the pulmonary vascular tree using pulmonary arterial lesions collected at pulmonary endarterectomy (PEA). We focused on the angiogenic vascular endothelial growth factor (VEGF)-A/VEGF receptor-2 (VEGFR2) axis and collagen 15A1 (COL15A1), a potential marker of endothelial cells of the systemic circulation. In parallel, we investigated *in vitro* angiogenic properties and barrier function of PAECs isolated from large and segmental pulmonary arterial lesions.

Results. Segmental pulmonary arterial lesions were abundantly recanalised by neovessels, paralleled by an enriched expression of VEGFR2. VEGF-A expression was more prominent in large pulmonary arterial lesions. However, we did not observe any significant difference in *in vitro* angiogenic capacities and barrier function of PAECs isolated from large and segmental pulmonary arterial lesions. Interestingly, we found the presence of endothelial cells ($CD31^+$) expressing COL15A1, but also $CD31^+$ cells which do not express COL15A1, suggesting that endothelial cells both from systemic and pulmonary circulation contribute to lesions recanalization.

Conclusion. Despite different *in situ* angiogenic cues in VEGF-A/VEGFR2 axis between large and segmental pulmonary arterial lesions in CTEPH, *in vitro* angiogenic capacities and barrier function remain unchanged.

INTRODUCTION

Chronic thromboembolic pulmonary hypertension (CTEPH) is a rare complication of massive or recurrent pulmonary embolism (1–3). It is characterised by intra-luminal unresolved thrombi associated with fibrous stenosis that partially or completely obstructs large pulmonary arteries. This eventually results in increased pulmonary vascular resistance (PVR), progressive pulmonary hypertension (PH), right ventricular (RV) failure and death, if left untreated (2,4,5). Additionally, CTEPH is associated with progressive microvasculopathy, including remodelling and obstruction of pulmonary microvessels in perfused and non-perfused areas (4,6,7), and enlargement of bronchial systemic vessels (8). The treatment of choice remains surgical removal of the fibro-thrombotic material, which is called pulmonary endarterectomy (PEA) (9).

Despite the identification of various risk factors -including persistent pulmonary embolism, venous thromboembolism, inflammatory diseases, splenectomy, non-O blood group, cancer, insufficient anticoagulation, increased antiphospholipid antibodies and lupus anticoagulant (4,10)- increasing the likelihood of CTEPH development, the precise sequence of cellular and molecular mechanisms leading to sustained fibro-thrombotic obstruction remains to be fully understood. Several hypotheses have been explored, including i) dysregulated thrombolysis (11–14); ii) inflammatory thrombosis (11,15–21); iii) activation of pulmonary artery endothelial (PAECs), smooth muscle (PASMCs), and progenitor cells (22–25); and iv) deficient angiogenesis (26–31). Previous research showed that angiogenesis is a key player in thrombus resolution and neovascularization, which is associated with CTEPH outcome (18,32). Moreover, we found that deficient angiogenesis plays a crucial role in the progression to CTEPH, as shown in our recent and unique CTEPH rabbit model (33) and described the 2-faced nature of angiogenesis in our recent review (34). Furthermore, PAECs isolated from PEA material were found to have reduced angiogenic properties compared to donor PAECs, suggesting their potential contribution to CTEPH pathophysiology (35).

Interestingly, several histological analyses of the pulmonary vascular lesions have previously evidenced differences in cellular and extracellular matrix composition along the pulmonary vascular tree, with notable variations observed in the degree of neovascularization across the lesion (15,16,18). It was suggested that these disparities could attributable to differences in flow dynamics, *e.g.* high-shear stress upstream of the occlusion, contrasting with low-shear stress and disrupted blood flow downstream of the occlusion (4). In addition, markers of the angiogenic signalling including vascular endothelial growth factor A (VEGF-A) or vascular endothelial growth factor receptor 2 (VEGFR2) are differentially expressed in fresh versus organized thrombi from PEA material (36). Recently, COL15A1 has been identified by Schupp *et al.* as a potential marker of a subpopulation of systemic endothelial cells (37). However, whether *in situ* expression patterns of endothelial and/or angiogenic markers along the pulmonary vascular tree could be explained by angiogenic behaviour or barrier function of PAECs remains unexplored.

Thus, we hypothesized that *in vitro* PAEC phenotype and function might differ depending on their location along the pulmonary vascular lesion tree from CTEPH patients. In the present study, we explored histological characteristics of pulmonary arterial lesions collected during PEA procedures and investigated *in vitro* angiogenic capacities and barrier function of PAECs according to their location along the pulmonary vascular tree in CTEPH patients.

MATERIALS AND METHODS

Study population

In this study, 8 patients diagnosed with CTEPH who underwent PEA at University Hospital Leuven between August 2018 and April 2023 and from whom endothelial cells were isolated, were included. The study protocol was approved by the Institutional Ethics Committee of the University Hospital of Leuven (S57114) and participants gave written informed consent.

Tissue collection

Pulmonary vascular lesions were collected at the time of PEA and the pulmonary vascular tree was reconstructed with the help of the surgeon. A specimen is shown in **Figure 1**. A piece from the large (upstream pulmonary vascular occlusion) and segmental/subsegmental (downstream pulmonary vascular occlusion) pulmonary artery, free from thrombotic material, was collected separately in endothelial growth medium MV2 (PromoCell) supplemented with 100 $U.mL^{-1}$ penicillin, 100 $\mu g.ml^{-1}$ 100 $\mu g.mL^{-1}$ streptomycin and 1.25 $\mu g.mL^{-1}$ amphotericin B (Life Technologies).

Histological assessment

A piece of large and segmental pulmonary arterial lesions was fixed in 4% paraformaldehyde and embedded in paraffin blocks. Five-µm thickness serial sections were deparaffinised and rehydrated. Collagen fibres, fibrin and muscle fibres were stained using Masson's Trichrome staining. Briefly, slides were fixed in Bouin's solution overnight and stained with working Weigert's iron hematoxylin, Biebrich scarlet-acid fuchsin, phosphotungstic/phosphomolybdic acid, aniline blue and acetic acid solutions, respectively. To explore endothelial markers and angiogenic signalling, immunolabelling with mouse monoclonal antibodies against CD31 (1:50, clone JC70A; Dako), and VEGF-A (1:100; clone VG-1; Abcam), rabbit monoclonal antibodies against VEGFR2 (1:200, clone 55b11, Cell Signalling) and rabbit polyclonal antibodies against COL15A1 (1:200, Invitrogen) was performed. Immunolabelling was revealed using horseradish peroxidase-conjugated goat-anti-mouse (1:1, Abcam) secondary antibodies for CD31 and VEGF-A, and horseradish peroxidase-conjugated goat-anti-rabbit (1:1, Abcam) secondary antibodies for VEGFR2 and COL15A1, and DAB substrate kit (Abcam) according to manufacturer's instructions. Nuclei were counterstained with hematoxylin. Pictures were taken using Axio Scan.Z1 (Zeiss) at 20x magnification. DAB-positive regions (positive pixels per total amount of pixels) were quantified using the open-source software QuPath (https://qupath.github.io). Only patients with at least one section of both large and segmental pulmonary arterial lesions were included for quantification. Due to technical reasons, patient cohort was reduced to n=4 for CD31 and COL15A1 and n=6 for VEGF-A and VEGFR2.

Isolation and purification of PAECs

PAECs were isolated from large and segmental pulmonary arterial lesions by collagenase I (1 $mg.mL^{-1}$, Gibco) digestion for 20 min and 30 min at 37°C, respectively (23,38). Cells were seeded onto gelatine-coated (2 mg/mL; Sigma-Aldrich) flasks in endothelial growth medium MV2 (PromoCell) supplemented with 100 $U.mL^{-1}$ penicillin, 100 $\mu g.mL^{-1}$ streptomycin and 1.25 $\mu g.mL^{-1}$ amphotericin B (Life Technologies) and maintained in culture at 37°C, 5% CO_2 and 95% humidity. To achieve homogenous populations of PAECs, cells were purified by immunomagnetic separation using anti-CD31 monoclonal antibody-labelled beads, according to manufacturer's instructions (Miltenyi Biotec). Before each experiment, PAECs were starved with basal endothelial medium MV2 (Promocell) containing 3.2% endothelial growth medium,

supplemented with 100 U.mL^{-1} penicillin, 100 µg.mL^{-1} streptomycin and 1.25 µg.mL^{-1} amphotericin B. All experiments were carried out with PAECs between passages 3 and 8.

Cell phenotyping

PAECs (3.000 cells/chamber) were seeded onto fibronectin-coated (10 µg.mL^{-1}; R&D Systems) 4-chamber slides (Nunc). PAECs were immunolabelled using primary mouse monoclonal antibodies against CD31 (1:25; clone JC70A; Dako) and vWF (1:50; clone F8/86; Dako), rabbit monoclonal antibodies against VE-cadherin (1:600; clone D87F2; Cell Signaling Technology), and Alexa fluor-594 goat anti-mouse (1:2000; Life Technologies) for CD31 and vWF and Alexa fluor-488 goat anti-rabbit (1:2000; Life Technologies) for VE-cadherin secondary antibodies, as previously described. Nuclei were stained with DAPI. Labelling of endothelial scavenger receptors was performed using dil-Ac-LDL (1:20; Tebubio), as previously described (38–40). All fluorescent images were taken at a 40x magnification using Olympus BX-UCB microscope equipped with X-Cite series 120Q (Excelitas Technologies).

Migration assay

PAECs were seeded onto gelatin-coated 2-well culture inserts (Ibidi, 81176) at a density of 7.500 cells/well (41). Confluent PAECs were starved for 6 h, inserts were removed and PAECs were placed in fresh endothelial growth medium and pictures were taken every 2 h for 20 h using EVOS Cell Imaging System (Thermo Fisher Scientific) equipped with EVOS Onstage Incubator (37°C, 5% CO2 and 95% humidity; Thermo Fisher Scientific). At each time point, the gap area was measured using ImageJ and subtracted from the initial gap area (baseline), further plotted over time, the area under the curve (AUC) was calculated and corresponds to migration velocity in mm^2.h^{-1}.

Tube formation assay

Angiogenesis µ-slide (Ibidi, 81506) was filled with Matrigel© (BD Bioscience) and incubated for 30 min at 37°C, as described elsewhere (41). PAECs were starved overnight, trypsinized, resuspended in endothelial growth medium and seeded on top of Matrigel© at a density of 5.000 cells/well. After 4 h incubation at 37°C, pictures were taken using EVOS Cell Imaging System. Number of nodes, junctions, branches and tubes was quantified in triplicate using 'Angiogenesis Analyzer' plug-in for ImageJ, created by Gilles Carpentier (42).

Barrier function assay

PAECs (10.000 cells/insert) suspended in growth medium were seeded onto gelatin-coated inserts of 24-well Transwell (Corning) (41,43). After 24 h, cells were starved overnight, and fluorescein isothiocyanate (FITC)-labelled bovine serum albumin (BSA) (0.1 mg.mL^{-1}; Sigma Aldrich) in starvation medium was added to the upper chamber, while the lower chamber was filled with starvation medium. Leakage of FITC-BSA through PAECs monolayer was assessed by collecting medium from the lower chamber at 30 min, 1, 2 and 4 h. Absorbance was measured (excitation 488 nm; emission 520 nm) using Synergy H1 hybrid reader (Biotek, Santa Clara) and Gen5 Software (Biotek). Leakage of FITC-BSA through PAECs monolayer was plotted over time and AUC was calculated and corresponds to leakage velocity in µg.mL^{-1}.h$^{-1.}$

Statistical analysis

Statistical analyses were performed using Graphpad Prism (version 9; GraphPad Software Inc.). Normality was checked using Shapiro-Wilk test. Differences between two groups were analysed using paired Student or Wilcoxon t-test, and 2-way multiple comparison ANOVA

followed by post-hoc Šídák's test. A p-value of <0.05 was considered statistically significant. Data shown are expressed as median (25^{th}-75^{th} interquartile range) in graphs and as mean ± SD or indicated otherwise within the text.

RESULTS

Histomorphometry of large and segmental pulmonary arterial lesions from CTEPH patients

Histological features along the pulmonary vascular tree, collagen and muscle fibres' content and expression of endothelial (CD31, COL15A1) and angiogenic markers (VEGF-A and VEGFR2) were explored in sections of large and segmental pulmonary arterial lesions (**Figure 2, 3**). Large pulmonary arterial lesions consist of media, with several layers of smooth muscle cells, and neointima with spindle-shaped cells, potentially myofibroblast-like cells (**Figure 2**). Segmental pulmonary arterial lesions (**Figure 3**) comprise a large amount of dense collagen fibres, with numerous recanalising vessels. $CD31^+$ recanalising vessels are more profuse in segmental (**Figure 3**) compared to large pulmonary arteries (**Figure 2**), as evidenced by a significantly larger $CD31^+$ area within segmental compared to large pulmonary arterial lesions (1.65 ± 1.17% vs. 5.60 ± 1.11%; p = 0.0163) (**Figure 4**). Interestingly, some $CD31^+$ recanalising vessels expressed COL15A1, a marker of ECs from the systemic circulation, whereas a substantial amount did not (**Figure 3; Figure S1**). This suggests that vessels recanalising fibro-thrombotic lesions may arise from either the bronchial circulation or the pulmonary circulation. Of note, $CD31^+$ cells lining the lumen of the obstructed segmental pulmonary arterial lesions do not express COL15A1 (**Figure S2**). Surprisingly, within the large pulmonary arterial wall, $CD31^-$ myofibroblast-like cells do express COL15A1 (**Figure 2**). Overall, the $COL15A1^+$ area tended to be higher in the large compared to segmental pulmonary arterial lesions (18.33 ± 10.70% vs. 4.72 ± 3.52%; p = 0.0525; **Figure 4**), probably because of the abundant presence of $COL15A1^+$ myofibroblast-like cells within large pulmonary arterial lesions. VEGF-A is expressed in both large and segmental pulmonary arterial lesions, with a significantly higher expression in large pulmonary arterial lesions (25.96 ± 16.61% vs. 7.72 ± 7.93%; p = 0.0260; **Figure 4**). In addition, neointimal myofibroblast-like cells and $CD31^-$ cells lining the lumen of large pulmonary arterial lesions express VEGF-A (**Figure 2**), whereas within segmental pulmonary arterial lesions, $CD31^+$ cells lining recanalising vessels do not express VEGF-A (**Figure 3**). Finally, VEGFR2 is expressed by myofibroblast-like cells in large pulmonary arterial lesions (**Figure 2**); in segmental pulmonary arterial lesions VEGFR2 is expressed by medial cells of recanalizing vessels, probably smooth muscle cells (**Figure 3**). However, no significant difference was observed in VEGFR2 expression between large and segmental pulmonary arterial lesions (13.51% [7.29-18.56%] vs. 17.74% [16.94-30.97%], median [interquartile range]; p = 0.2188; **Figure 4**).

In vitro angiogenic capacity of ECs from large and segmental pulmonary arterial lesions

Considering the differences observed in the VEGF-A/VEGFR2 signalling pathway expression between large and segmental pulmonary arterial lesions, we aim to assess whether *in vitro* angiogenic properties of large and segmental pulmonary arterial lesions would be differently affected. Consequently, PAECs isolated from large and segmental pulmonary arterial lesions were phenotyped, as illustrated in **Figure 5**. Both display a typical "cobblestone" morphology and establish a homogenous monolayer (**Figure 5a & 5b**). Both large and segmental PAECs express CD31 (**Figure 5c & 5d)** and VE-cadherin (**Figure 5e & 5f)** at their surface, vWF (**Figure 5g & 5h)** in their cytoplasm and take up acetylated LDL (**Figure 5i & 5j)** via

endothelium-specific scavenger receptors. *In vitro* angiogenic capacity was assessed by performing migration and tube formation assays in PAECs from both large and segmental pulmonary arterial lesions. Wound closure time (**Figure 6a)** and averaged migration area do not significantly differ over time (6 h: 1.29 ± 0.37 mm^2/h vs. 1.32 ± 0.35 mm^2/h; p = 0.99; 12 h: 2.25 ± 0.27 mm^2/h vs. 2.35 ± 0.24 mm^2/h; p = 0.93; 18 h: 2.45 ± 0.11 mm^2/h vs. 2.56 ± 0.22 mm^2/h; p = 0.75; and 20 h: 2.48 ± 0.12 mm^2/h vs. 2.56 ± 0.22 mm^2/h; p = 0.90) between large and segmental PAECs (**Figure 6b**). Accordingly, migration velocity of large and segmental PAECs does not significantly differ (34 ± 3.4 mm^2/h vs. 35 ± 3.7 mm^2/h; p = 0.34) (**Figure 6c**). Averaged number of nodes (533 ± 234 vs. 484 ± 165; p = 0.49), segments 187 ± 95 vs. 165 ± 66; p = 0.45), junctions (152 ± 66 vs. 139 ± 46; p = 0.51) and branches (83 ± 10 vs. 83 ± 9; p = 0.90) do not significantly differ between large and segmental PAECs (**Figure 7a-e**). These findings indicate that *in vitro* angiogenic capacities do not differ between ECs from large and segmental pulmonary lesions of CTEPH patients.

Barrier function of ECs from large and segmental pulmonary arteries

Knowing that various vascular pathologies are associated with impaired barrier function (44) and inflammatory cell infiltration was observed in pulmonary arterial lesions from CTEPH patients (18), we aimed to investigate whether *in vitro* endothelial barrier function could be differently affected in large and segmental pulmonary arterial lesions from CTEPH patients. BSA-FITC leakage through the endothelial monolayer over time does not significantly differ between PAECs from large and segmental pulmonary lesions, (30 min: 0.26 ± 0.12 µg/mL vs. 0.25 ± 0.08 µg/mL; p > 0.99; 1 h: 0.46 ± 0.18 µg/mL vs. 0.49 ± 0.12 µg/mL; p > 0.99; 2 h: 0.81 ± 0.34 µg/mL vs. 0.84 ± 0.21 µg/mL; p > 0.99; 4 h: 1.18 ± 0.44 µg/mL vs. 1.32 ± 0.29 µg/mL; p = 0.96; **Figure 8a**). Likewise, BSA-leakage velocity does not significantly differ between large and segmental PAECs (1.53 µg/mL/h [1.30-1.75 µg/mL/h] vs. 1.60 µg/mL/h [1.48-2.04 µg/mL/h], median [interquartile range]; p = 0.74; **Figure 8b**). These results indicate that the endothelial barrier function is similarly affected in large and segmental pulmonary lesions from CTEPH patients.

DISCUSSION

In this article, we observed differences in *in situ* angiogenic cues of the VEGF-A/VEGFR2 axis, whereas *in vitro* angiogenic capacities and endothelial barrier function did not significantly differ according to the location (large vs. segmental) along the pulmonary vascular lesion tree. Interestingly, we found that only a proportion of vessels recanalising segmental pulmonary arterial lesions express COL15A1, a marker of systemic endothelial cells (37); this suggests that the source of endothelial cells within vessels recanalising pulmonary arterial lesions in CTEPH patients is diverse and may involve ECs from both systemic and pulmonary circulation or even progenitor ECs.

In the present study, we found that both large and segmental pulmonary arterial lesions contain muscle and collagen fibres. In large pulmonary arterial lesions, numerous myofibroblast-like cells are present in the neointima, evidence of intense vascular remodelling, as previously described (16,17,36). The presence of myofibroblast-like cells may result from Endothelial-to-Mesenchymal transition (EndoMT), which could further contribute to the formation of fibro-thrombotic material obstructing pulmonary arteries in CTEPH (45,46). Interestingly, Bocheneck et al. have previously shown that TGFβ1 signalling, known to promote EndoMT, prevents venous thrombus resolution potentially contributing to CTEPH pathogenesis (47,48).

COL15A1 is a member of the multiplexin superfamily of collagens, produced by fibroblasts, smooth muscle cells and endothelial cells (49,50). Its main function is organizing, stabilizing and integrating the basement membrane to underlying connective tissue (49). Recently, COL15A1 was identified by Schupp et al. as a specific marker of systemic endothelial cells in control human lung using single-cell RNA sequencing (37). Within segmental recanalised pulmonary arterial lesions, we observed both $CD31^{+}COL15A1^{+}$ cells, but also $CD31^{+}COL15A1^{-}$ cells; in addition, we found that PAECs lining the pulmonary arterial lumen are $CD31^{+}COL15A1^{-}$. These findings suggest that that vessels recanalising fibro-thrombotic lesions may arise from the bronchial circulation, as previously proposed (51) but also from the pulmonary circulation; in addition, this does not rule out the potential involvement of progenitor cells (25,52,53). Surprisingly, within large pulmonary arterial lesions, $CD31^{-}$ myofibroblast-like cells do express COL15A1, suggesting either involvement of EndoMT as abovementioned or smooth muscle dedifferentiation, as often seen in neointima formation.

Considering that angiogenesis is a key player in thrombus resolution (34) in CTEPH progression as recently shown in our CTEPH rabbit model (33), and can affect outcome in CTEPH patients (18), the angiogenic VEGF-A/VEGFR2 axis understandably emerged as a potential contributor.
VEGF-A is expressed in both large and segmental pulmonary arterial lesions, with a greater level in large pulmonary arterial lesions, which may appear counter-intuitive considering the large presence of recanalising vessels in segmental pulmonary arterial lesions. Within segmental pulmonary arterial lesions, $CD31^{+}$cells lining recanalising vessels do not express VEGF-A, suggesting that other ligands such as VEGF-C or VEGF-D could be involved, although their binding affinity is weaker compared to VEGF-A, or VEGF-B and placenta growth factor (PIGF) via VEGFR1 (54). By contrast, Bochenek et al. previously found that the endothelium of vessels recanalising lesions do express VEGF (36), although VEGF type was not clearly mentioned. Finally, VEGFR2 is expressed by myofibroblast-like and medial smooth muscle cells in pulmonary arterial lesions, without any significant difference between large and segmental pulmonary arterial lesions. Accordingly, Bochenek et al. also found VEGFR2 expression in spindle-shaped cells within organized thrombi and myofibroblasts (36).

To further elucidate, the differential features of the angiogenic VEGF-A/VEGFR2 axis observed between large and segmental pulmonary arterial lesions, we aim to investigate their *in vitro* angiogenic properties, knowing that migration and tube formation capacity of PAECs from PEA material can be impaired, in comparison with control PAECs from healthy donors (35). However, we did not find any difference between PAECs from large and segmental lesions. These findings are not in line with the $CD31^{+}$ high content and the numerous recanalising vessels observed in segmental pulmonary arterial lesions. Nevertheless, we should consider that PAECs were isolated from PEA material of CTEPH patients at rather advanced disease stages of the disease; consequently, gaining cells at diagnosis via right heart catheterization (39) could be an alternative approach to overcome this aspect. In addition, angiogenic capacities are measured using Matrigel©, which composition is far different from the *in vivo* extracellular matrix.

In addition to resulting in altered angiogenic properties, imbalance of the VEGF-A/VEGFR2 axis can also affect vascular permeability and endothelial cell function (54). In vascular pathology such as CTEPH, the role of the endothelium is pivotal as it governs the movement of circulating proteins and cells between the bloodstream and the underlying tissues. Actually, we previously showed that inflammatory triggers impair endothelial integrity in the context of pulmonary hypertension (43) and observed inflammatory cell accumulation (T-lymphocytes,

macrophage and neutrophils) in PEA material of CTEPH patients (18). Moreover, ischemia and changes in shear stress can alter endothelial barrier function (56–58). However, we did not observe any significant difference in barrier function between large and segmental PAECs, suggesting that endothelial barrier function is equally impaired in both vascular beds.

Several limitations would deserve to be mentioned. The authors are aware that the *in vitro* results are based on primary cells maintained in culture; despite the use of a standardized isolation protocol, it cannot be excluded that a biased selection of the most robust cell clusters does occur. As abovementioned, cells were isolated from PEA material obtained from patients at already advanced stages of the disease; this does not illustrate the cell potential at early phases, after an acute episode of pulmonary embolism. Lastly, the use of synthetic hydrogel in simplified 2D *in vitro* assays, in absence of blood flow and shear-stress conditions does not fully replicate the *in vivo* conditions and bypass interactions between cells and the extracellular matrix.

In conclusion, both systemic and pulmonary endothelial cells contribute to the recanalization of fibro-thrombotic pulmonary vascular lesions in CTEPH patients. Despite different *in situ* angiogenic cues in VEGF-A/VEGFR2 axis according to the location along the pulmonary vascular tree, *in vitro* angiogenic capacities and barrier function remain unchanged, suggesting that simplified *in vitro* assays are probably not completely adequate to explain all *in situ* features. Consequently, the emergence of more sophisticated *in vitro* systems such as organoids and microfluidic devices, in which cells and organ-derived ECM could be combined, should contribute to elucidating the mechanisms potentially involved.

ACKNOWLEDGEMENTS

The authors would like to the Belgian Association of Patients for Pulmonary Hypertension (Belgische Pulmonale Hypertensie Patiëntenvereniging) for its financial support.

Conflict of interests: MD received financial support from the Belgian Association of Patients for Pulmonary Hypertension.

Funding: This work was supported by research grants from the “Fonds voor Wetenschappelijk Onderzoek Vlaanderen” (G061123N) and Internal Funds from University of Leuven (C24E-21-032). LW is holder of a fellowship in the framework of Global PhD Partnerships between Leuven and Leiden Universities (GPUL/20/010).

Ethical approval: The study protocol was approved by the Institutional Ethics Committee of the University Hospital of Leuven (S57114).

Guarantor: not applicable

Author contributions: RQ conceived and designed the study, contributed to data interpretation, reviewed the manuscript; JV and LW collected the data, performed data analysis and interpretation; drafted the manuscript. AW, RS, ND and LA collected data and reviewed the manuscript. TV and MD collected patient material and reviewed the manuscript; all authors approved the final version.

REFERENCES

1. Delcroix M, Torbicki A, Gopalan D, Sitbon O, Klok FA, Lang I, et al. ERS statement on chronic thromboembolic pulmonary hypertension. Eur Respir J. 2021;57:2002828.

2. Humbert M, Kovacs G, Hoeper MM, Badagliacca R, Berger RMF, Brida M, et al. 2022 ESC/ERS Guidelines for the diagnosis and treatment of pulmonary hypertension. Eur Respir J. 2022;63:2200879.
3. Klok FA, Couturaud F, Delcroix M, Humbert M. Diagnosis of chronic thromboembolic pulmonary hypertension after acute pulmonary embolism. Eur Respir J. 2020;55:2000189.
4. Simonneau G, Torbicki A, Dorfmüller P, Kim N. The pathophysiology of chronic thromboembolic pulmonary hypertension. Eur Respir Rev. 2017;26:160112.
5. Kim NH, Delcroix M, Jais X, Madani MM, Matsubara H, Mayer E, et al. Chronic thromboembolic pulmonary hypertension. Eur Respir J. 2019;53:1801915.
6. Galie N. Pulmonary Microvascular Disease in Chronic Thromboembolic Pulmonary Hypertension. Proc Am Thorac Soc. 2006;3:571–6.
7. Moser KM, Bloor CM. Pulmonary vascular lesions occurring in patients with chronic major vessel thromboembolic pulmonary hypertension. Chest. 1993;103:685–92.
8. Dorfmüller P, Günther S, Ghigna MR, Thomas de Montpréville V, Boulate D, Paul JF, et al. Microvascular disease in chronic thromboembolic pulmonary hypertension: a role for pulmonary veins and systemic vasculature. Eur Respir J. 2014;44:1275–88.
9. Jenkins D. Pulmonary endarterectomy: the potentially curative treatment for patients with chronic thromboembolic pulmonary hypertension. Eur Respir Rev. 2015;24:263–71.
10. Elwing JM, Vaidya A, Auger WR. Chronic Thromboembolic Pulmonary Hypertension: An Update. Clin Chest Med. 2018;39:605–20.
11. Kim NH, Lang IM. Risk factors for chronic thromboembolic pulmonary hypertension. Eur Respir Rev. 2012;21:27–31.
12. Lang IM, Pesavento R, Bonderman D, Yuan JXJ. Risk factors and basic mechanisms of chronic thromboembolic pulmonary hypertension: a current understanding. Eur Respir J. 2013;41:462–8.
13. Manz XD, Szulcek R, Pan X, Symersky P, Dickhoff C, Majolée J, et al. Epigenetic Modification of the von Willebrand Factor Promoter Drives Platelet Aggregation on the Pulmonary Endothelium in Chronic Thromboembolic Pulmonary Hypertension. Am J Respir Crit Care Med. 2022;205:806–18.
14. Manz XD, Bogaard HJ, Aman J. Regulation of VWF (Von Willebrand Factor) in Inflammatory Thrombosis. Arterioscler Thromb Vasc Biol. 2022;42:1307–20.
15. Arbustini E, Morbini P, D'Armini AM, Repetto A, Minzioni G, Piovella F, et al. Plaque composition in plexogenic and thromboembolic pulmonary hypertension: the critical role of thrombotic material in pultaceous core formation. Heart Br Card Soc. 2002 Aug;88(2):177–82.
16. Bernard J, Yi ES. Pulmonary thromboendarterectomy: a clinicopathologic study of 200 consecutive pulmonary thromboendarterectomy cases in one institution. Hum Pathol. 2007;38:871–7.
17. Blauwet LA, Edwards WD, Tazelaar HD, McGregor CGA. Surgical pathology of pulmonary thromboendarterectomy: a study of 54 cases from 1990 to 2001. Hum Pathol. 2003;34:1290–8.
18. Quarck R, Wynants M, Verbeken E, Meyns B, Delcroix M. Contribution of inflammation and impaired angiogenesis to the pathobiology of chronic thromboembolic pulmonary hypertension. Eur Respir J. 2015;46:431–43.
19. Kimura H, Okada O, Tanabe N, Tanaka Y, Terai M, Takiguchi Y, et al. Plasma Monocyte Chemoattractant Protein-1 and Pulmonary Vascular Resistance in Chronic Thromboembolic Pulmonary Hypertension. Am J Respir Crit Care Med. 2001;164:319–24.
20. Quarck R, Nawrot T, Meyns B, Delcroix M. C-Reactive Protein. J Am Coll Cardiol. 2009;53:1211–8.
21. Langer F, Schramm R, Bauer M, Tscholl D, Kunihara T, Schäfers HJ. Cytokine Response to Pulmonary Thromboendarterectomy. CHEST. 2004;126:135–41.
22. Wynants M, Vengethasamy L, Ronisz A, Meyns B, Delcroix M, Quarck R. NF-κB pathway is involved in CRP-induced effects on pulmonary arterial endothelial cells in chronic thromboembolic pulmonary hypertension. Am J Physiol-Lung Cell Mol Physiol. 2013;305:L934–42.

23. Wynants M, Quarck R, Ronisz A, Alfaro-Moreno E, Raemdonck DV, Meyns B, et al. Effects of C-reactive protein on human pulmonary vascular cells in chronic thromboembolic pulmonary hypertension. Eur Respir J. 2012;40:886–94.

24. Firth AL, Yao W, Ogawa A, Madani MM, Lin GY, Yuan JXJ. Multipotent mesenchymal progenitor cells are present in endarterectomized tissues from patients with chronic thromboembolic pulmonary hypertension. Am J Physiol Cell Physiol. 2010;298:C1217-1225.

25. Yao W, Firth AL, Sacks RS, Ogawa A, Auger WR, Fedullo PF, et al. Identification of putative endothelial progenitor cells (CD34+CD133+Flk-1+) in endarterectomized tissue of patients with chronic thromboembolic pulmonary hypertension. Am J Physiol Lung Cell Mol Physiol. 2009;296:L870-878.

26. Waltham M, Burnand KG, Collins M, McGuinness CL, Singh I, Smith A. Vascular endothelial growth factor enhances venous thrombus recanalisation and organisation. Thromb Haemost. 2003;89:169–76.

27. Waltham M, Burnand K, Fenske C, Modarai B, Humphries J, Smith A. Vascular endothelial growth factor naked DNA gene transfer enhances thrombus recanalization and resolution. J Vasc Surg. 2005;42:1183–9.

28. Modarai B, Humphries J, Gossage JA, Waltham M, Burnand KG, Kanaganayagam GS, et al. Adenovirus-Mediated VEGF Gene Therapy Enhances Venous Thrombus Recanalization and Resolution. Arterioscler Thromb Vasc Biol. 2008;28:1753–9.

29. Alias S, Redwan B, Panzenböck A, Winter MP, Schubert U, Voswinckel R, et al. Defective Angiogenesis Delays Thrombus Resolution: A Potential Pathogenetic Mechanism Underlying Chronic Thromboembolic Pulmonary Hypertension. Arterioscler Thromb Vasc Biol. 2014;34:810–9.

30. Evans CE, Grover SP, Humphries J, Saha P, Patel AP, Patel AS, et al. Antiangiogenic Therapy Inhibits Venous Thrombus Resolution. Arterioscler Thromb Vasc Biol. 2014;34:565–70.

31. Hobohm L, Kölmel S, Niemann C, Kümpers P, Krieg VJ, Bochenek ML, et al. Role of angiopoietin-2 in venous thrombus resolution and chronic thromboembolic disease. Eur Respir J. 2021;58:2004196.

32. Hosokawa K, Ishibashi-Ueda H, Kishi T, Nakanishi N, Kyotani S, Ogino H. Histopathological Multiple Recanalized Lesion Is Critical Element of Outcome After Pulmonary Thromboendarterectomy. Int Heart J. 2011;52:377–81.

33. Quarck R, Tielemans B, Willems L, Stoian L, Ronisz A, Wagenaar A, et al. Impairment of angiogenesis-driven clot resolution is a key event in the progression to CTEPH: validation in a novel rabbit model. Arterioscler Thromb Vasc Biol. 2023;43:1308–21.

34. Willems L, Kurakula K, Verhaegen J, Klok FA, Delcroix M, Goumans MJ, et al. Angiogenesis in Chronic Thromboembolic Pulmonary Hypertension: A Janus-Faced Player? Arterioscler Thromb Vasc Biol. 2024; DOI: ATVBAHA.123.319852.

35. Viswanathan G, Kirshner HF, Nazo N, Ali S, Ganapathi A, Cumming I, et al. Single-Cell Analysis Reveals Distinct Immune and Smooth Muscle Cell Populations that Contribute to Chronic Thromboembolic Pulmonary Hypertension. Am J Respir Crit Care Med. 2023;207:1358–75.

36. Bochenek ML, Rosinus NS, Lankeit M, Hobohm L, Bremmer F, Schütz E, et al. From thrombosis to fibrosis in chronic thromboembolic pulmonary hypertension. Thromb Haemost. 2017;117:769–83.

37. Schupp JC, Adams TS, Cosme C, Raredon MSB, Yuan Y, Omote N, et al. Integrated Single-Cell Atlas of Endothelial Cells of the Human Lung. Circulation. 2021;144:286–302.

38. Quarck R, Wynants M, Ronisz A, Sepulveda MR, Wuytack F, Van Raemdonck D, et al. Characterization of proximal pulmonary arterial cells from chronic thromboembolic pulmonary hypertension patients. Respir Res. 2012;13:27.

39. Tielemans B, Stoian L, Wagenaar A, Leys M, Belge C, Delcroix M, et al. Incremental Experience in In Vitro Primary Culture of Human Pulmonary Arterial Endothelial Cells Harvested from Swan-Ganz Pulmonary Arterial Catheters. Cells. 2021;10:3229.

40. Vengethasamy L, Hautefort A, Tielemans B, Belge C, Perros F, Verleden S, et al. BMPRII influences the response of pulmonary microvascular endothelial cells to inflammatory mediators. Pflüg Arch - Eur J Physiol. 2016;468:1969–83.

41. Tielemans B, Wagenaar A, Belge C, Delcroix M, Quarck R. Pulmonary arterial hypertension drugs can partially restore altered angiogenic capacities in bmpr2-silenced human lung microvascular endothelial cells. Pulm Circ. 2023;13:e12293.
42. Carpentier G. Angiogenic Analyzer [Internet]. Available from: http://image.bio.methods.free.fr/ImageJ/?Angiogenesis-Analyzer-for-ImageJ.
43. Tielemans B, Stoian L, Gijsbers R, Michiels A, Wagenaar A, Farre Marti R, et al. Cytokines trigger disruption of endothelium barrier function and p38 MAP kinase activation in BMPR2-silenced human lung microvascular endothelial cells. Pulm Circ. 2019;9:2045894019883607.
44. Park-Windhol C, D'Amore PA. Disorders of Vascular Permeability. Annu Rev Pathol. 2016;11:251–81.
45. Sakao S, Hao H, Tanabe N, Kasahara Y, Kurosu K, Tatsumi K. Endothelial-like cells in chronic thromboembolic pulmonary hypertension: crosstalk with myofibroblast-like cells. Respir Res. 2011;12:109.
46. Arciniegas E, Frid MG, Douglas IS, Stenmark KR. Perspectives on endothelial-to-mesenchymal transition: potential contribution to vascular remodeling in chronic pulmonary hypertension. Am J Physiol-Lung Cell Mol Physiol. 2007;293:L1–8.
47. Bochenek ML, Leidinger C, Rosinus NS, Gogiraju R, Guth S, Hobohm L, et al. Activated Endothelial TGFβ1 Signaling Promotes Venous Thrombus Nonresolution in Mice Via Endothelin-1. Circ Res. 2020;126:162–81.
48. Bochenek ML, Saar K, Nazari-Jahantigh M, Gogiraju R, Wiedenroth CB, Münzel T, et al. Endothelial Overexpression of TGF-β-Induced Protein Impairs Venous Thrombus Resolution. JACC Basic Transl Sci. 2024;9:100–16.
49. Myers JC, Dion AS, Abraham V, Amenta PS. Type XV collagen exhibits a widespread distribution in human tissues but a distinct localization in basement membrane zones. Cell Tissue Res. 1996;286:493–505.
50. Prockop DJ, Kivirikko KI. COLLAGENS: Molecular Biology, Diseases, and Potentials for Therapy. Annu Rev Biochem. 1995;64:403–34.
51. Dorfmüller P, Günther S, Ghigna MR, Montpréville VT de, Boulate D, Paul JF, et al. Microvascular disease in chronic thromboembolic pulmonary hypertension: a role for pulmonary veins and systemic vasculature. Eur Respir J. 2014;44:1275–88.
52. Nicklas JM, Gordon AE, Henke PK. Resolution of Deep Venous Thrombosis: Proposed Immune Paradigms. Int J Mol Sci. 2020;21:2080.
53. Alvarez DF, Huang L, King JA, ElZarrad MK, Yoder MC, Stevens T. Lung microvascular endothelium is enriched with progenitor cells that exhibit vasculogenic capacity. Am J Physiol-Lung Cell Mol Physiol. 2008;294:L419–30.
54. Shibuya M, Claesson-Welsh L. Signal transduction by VEGF receptors in regulation of angiogenesis and lymphangiogenesis. Exp Cell Res. 2006;312:549–60.
55. Tura-Ceide O, Smolders VFED, Aventin N, Morén C, Guitart-Mampel M, Blanco I, et al. Derivation and characterisation of endothelial cells from patients with chronic thromboembolic pulmonary hypertension. Sci Rep. 2021;11:18797.
56. Nagy JA, Benjamin L, Zeng H, Dvorak AM, Dvorak HF. Vascular permeability, vascular hyperpermeability and angiogenesis. Angiogenesis. 2008;11(2):109–19.
57. Weis SM. Vascular permeability in cardiovascular disease and cancer. Curr Opin Hematol. 2008;15:243–9.
58. Paszkowiak JJ, Dardik A. Arterial wall shear stress: observations from the bench to the bedside. Vasc Endovascular Surg. 2003;37:47–57.

FIGURES AND FIGURE LEGENDS

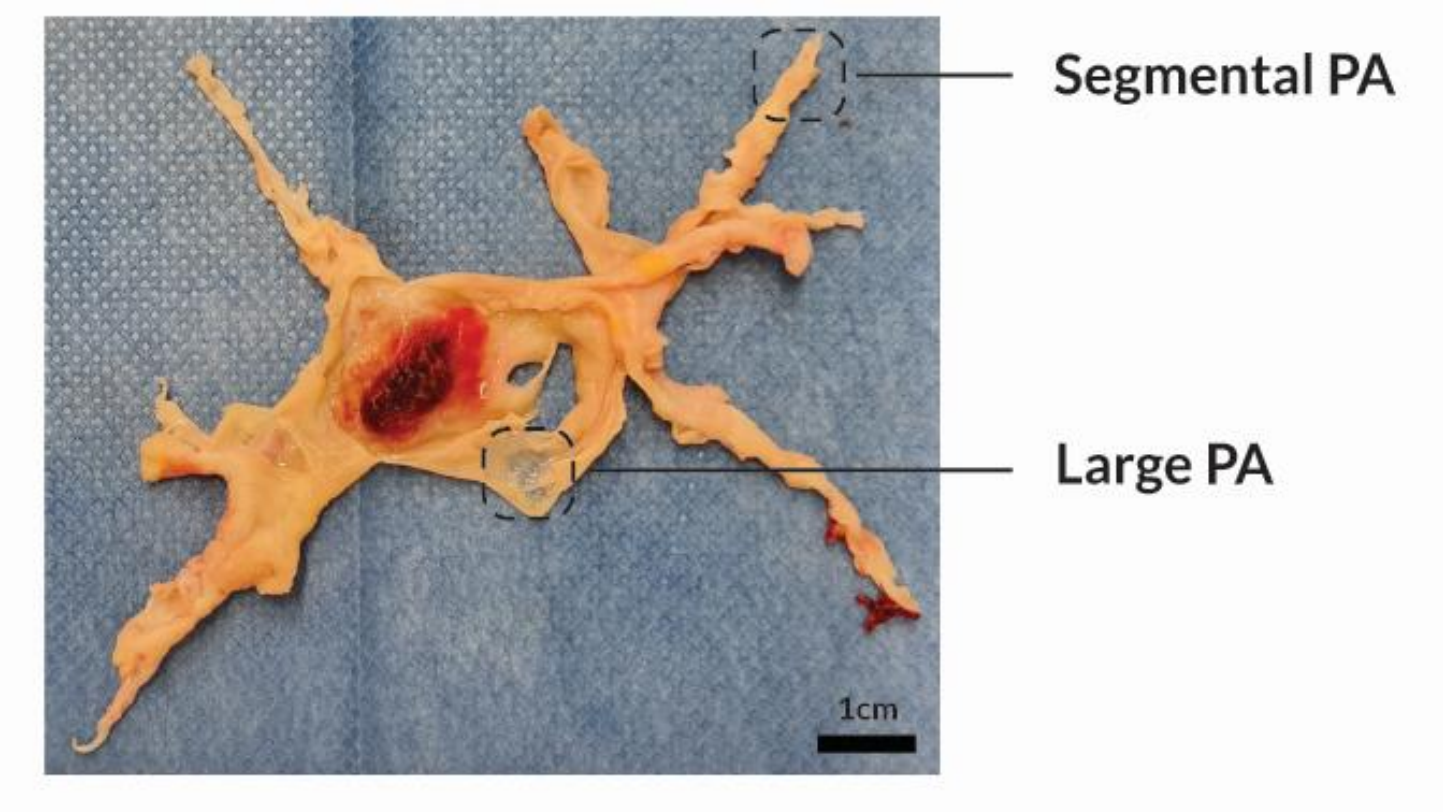

Figure 1: Representative resection specimen obtained during PEA. Fibro-thrombotic material obstructing pulmonary arteries is divided into large pulmonary artery, upstream the obstruction by thrombotic material, and segmental pulmonary artery, downstream the obstruction by thrombotic material. PA, pulmonary artery; PEA, pulmonary endarterectomy.

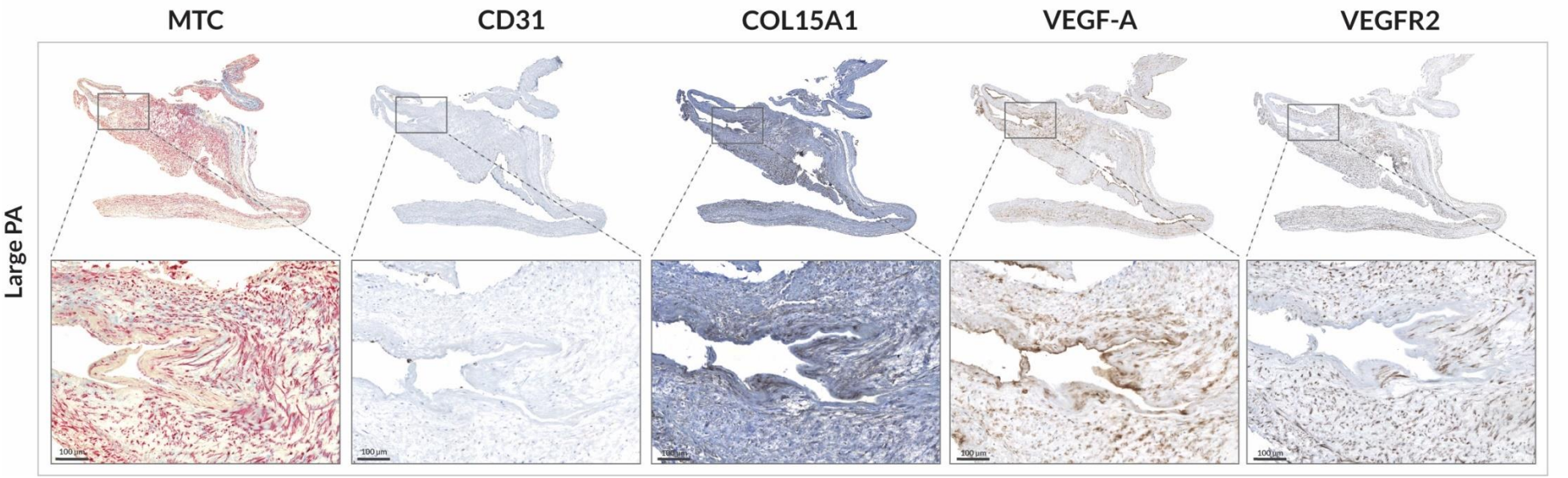

Figure 2: Histological evaluation of large pulmonary arterial lesions of CTEPH patients. Large pulmonary artery tissues were stained with Masson's trichrome stain (collagen, blue; muscle fibres, red) and immunolabelled using COL15A1, CD31, VEGF-A, and VEGFR2 antibodies. In total, PEA material of 8 patients was evaluated and similar lesions were observed. Scale bar = 100 µm. PA, pulmonary artery; PEA, pulmonary endarterectomy; MTC, Masson Trichrome; VEGF-A, Vascular endothelial growth factor A; VEGFR2, Vascular endothelial growth factor receptor 2.

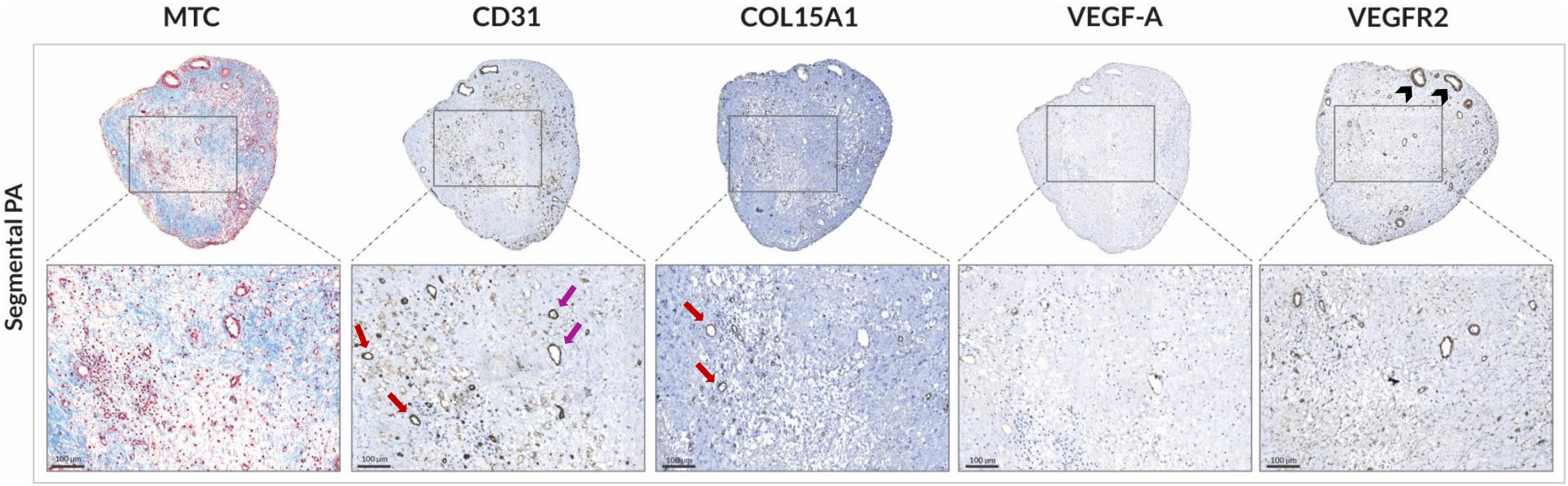

Figure 3: Histological evaluation of segmental pulmonary arterial lesions of CTEPH patients. Segmental pulmonary arterial lesions were stained with Masson's trichrome stain (collagen, blue; muscle fibres, red) and immunolabelled using COL15A1, CD31, VEGF-A, and VEGFR2 antibodies. In total, PEA material of 8 patients was evaluated and similar lesions were observed. Scale bar = 100 µm; purple arrow, $CD31^{+}$ recanalising vessel; red arrow, $CD31^{+}COL15A1^{+}$ recanalising vessel; arrowhead, $VEGFR2^{+}$ cells in media of recanalising vessel, potentially smooth muscle cells. PA, pulmonary artery; PEA, pulmonary endarterectomy; MTC, Masson Trichrome; VEGF-A, Vascular endothelial growth factor A; VEGFR2, Vascular endothelial growth factor receptor 2.

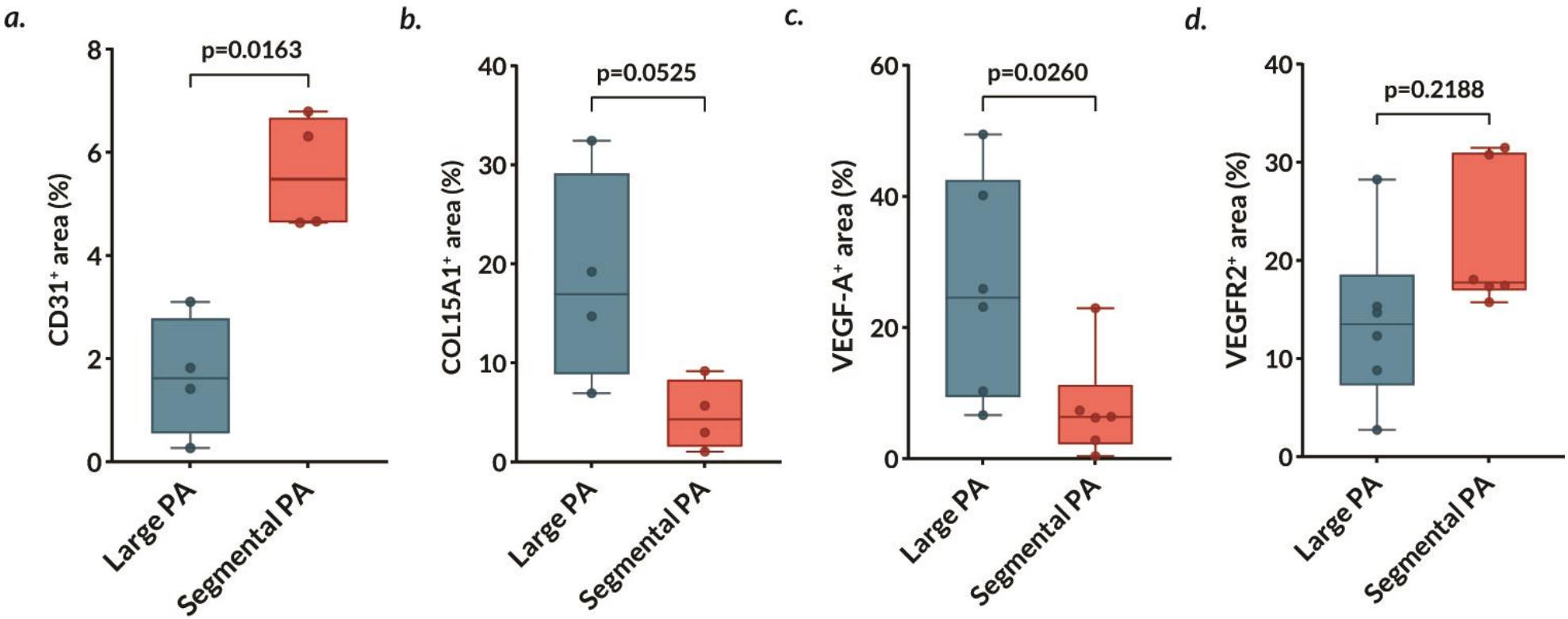

Figure 4: Quantification of endothelial and angiogenic signalling markers' pattern expression in large and segmental pulmonary arterial lesions of CTEPH patients. DAB-positive regions of CD31 (n=4), COL15A1 (n=4), VEGF-A (n=6) and VEGFR2 (n=6) expression in large and segmental pulmonary artery tissue were quantified using QuPath software. Due to technical reasons, patient cohort was reduced to n=4 for CD31 and COL15A1 and n=6 for VEGF-A and VEGFR2. Results are expressed as median (25^{th}-75^{th} interquartile range). Comparisons by paired Student and Wilcoxon t-test. PA, pulmonary artery; VEGF-A, vascular endothelial growth factor A; VEGFR2, vascular endothelial growth factor receptor 2.

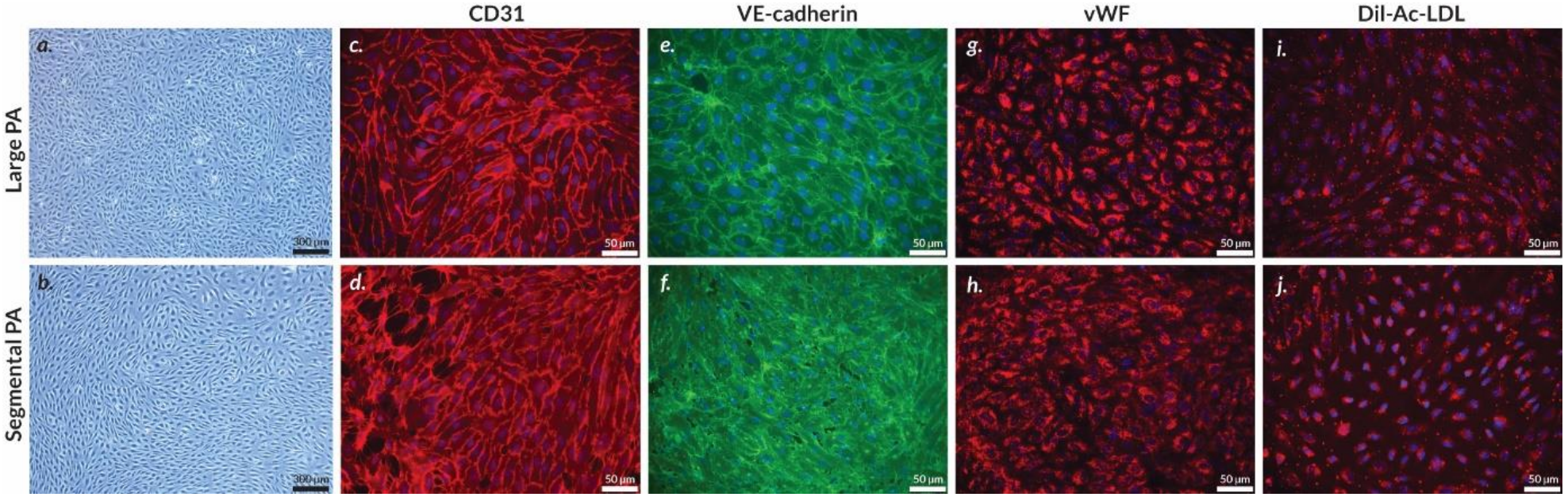

Figure 5: Phenotyping of PAECs from large and segmental pulmonary arterial lesions of CTEPH patients. Primary culture of large and segmental PAECs isolated from PEA material **(a,b)**. PAECs were characterised for endothelial phenotype by cell surface markers CD31**(c,d)** and VE-cadherin **(e,f)**, and intracellular endothelial marker vWF **(g,h)**. Endothelial phenotype was further confirmed by scavenger receptor capacity to internalize acetylated low-density-lipoprotein **(i,j)**. Nuclei were counterstained with DAPI (blue). Experiments were carried out between passages 3 and 7. Scale = 300 µm (**a,b**) and 50 µm (**c-j**). PAECs, pulmonary artery endothelial cells; PA, pulmonary artery; PEA, pulmonary endarterectomy; vWF, von Willebrand factor.

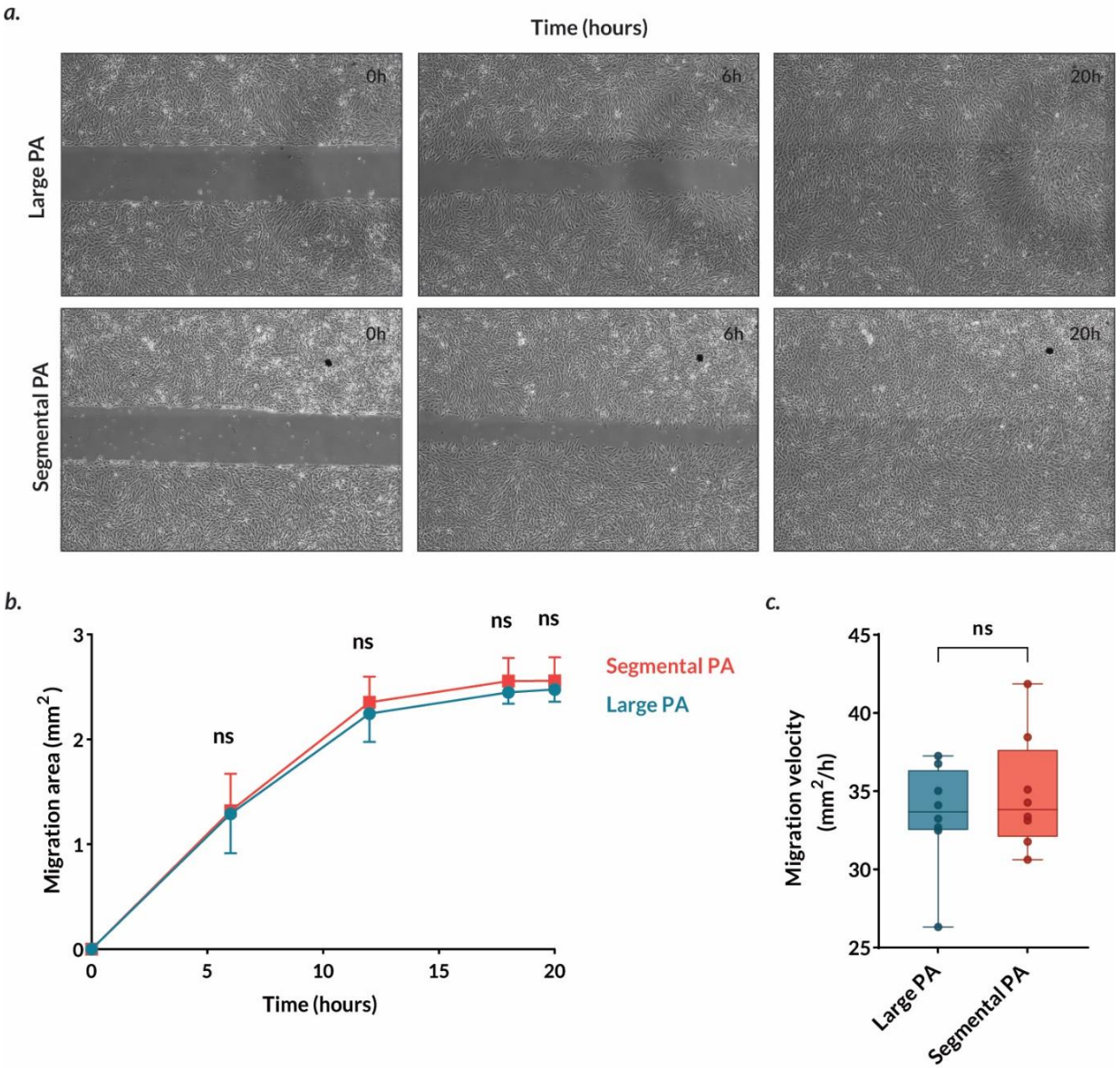

Figure 6: Migration capacity of PAECs isolated from large and segmental pulmonary arterial lesions of CTEPH patients. Representative pictures of wound closure over time of large and segmental PAECs **(a)**. Migration capacity of large and segmental PAECs was assessed by measuring the gap area over time. Representative time curve of mean migration area (mm^2) for large and segmental PAECs **(b)**. Migration velocity (mm^2/h) of large and segmental PAECs was assessed by measuring the area under the curve of the migration area **(c)**. Two independent experiments per patient (n=8) were carried out between passages 3 and 8 and expressed as median (25^{th}-75^{th} interquartile range). Comparisons by two-way ANOVA and post-hoc Šídák's test (**b**) and paired Student t-test (**c**). ns, non significant; PAECs, pulmonary artery endothelial cells; PA, pulmonary artery.

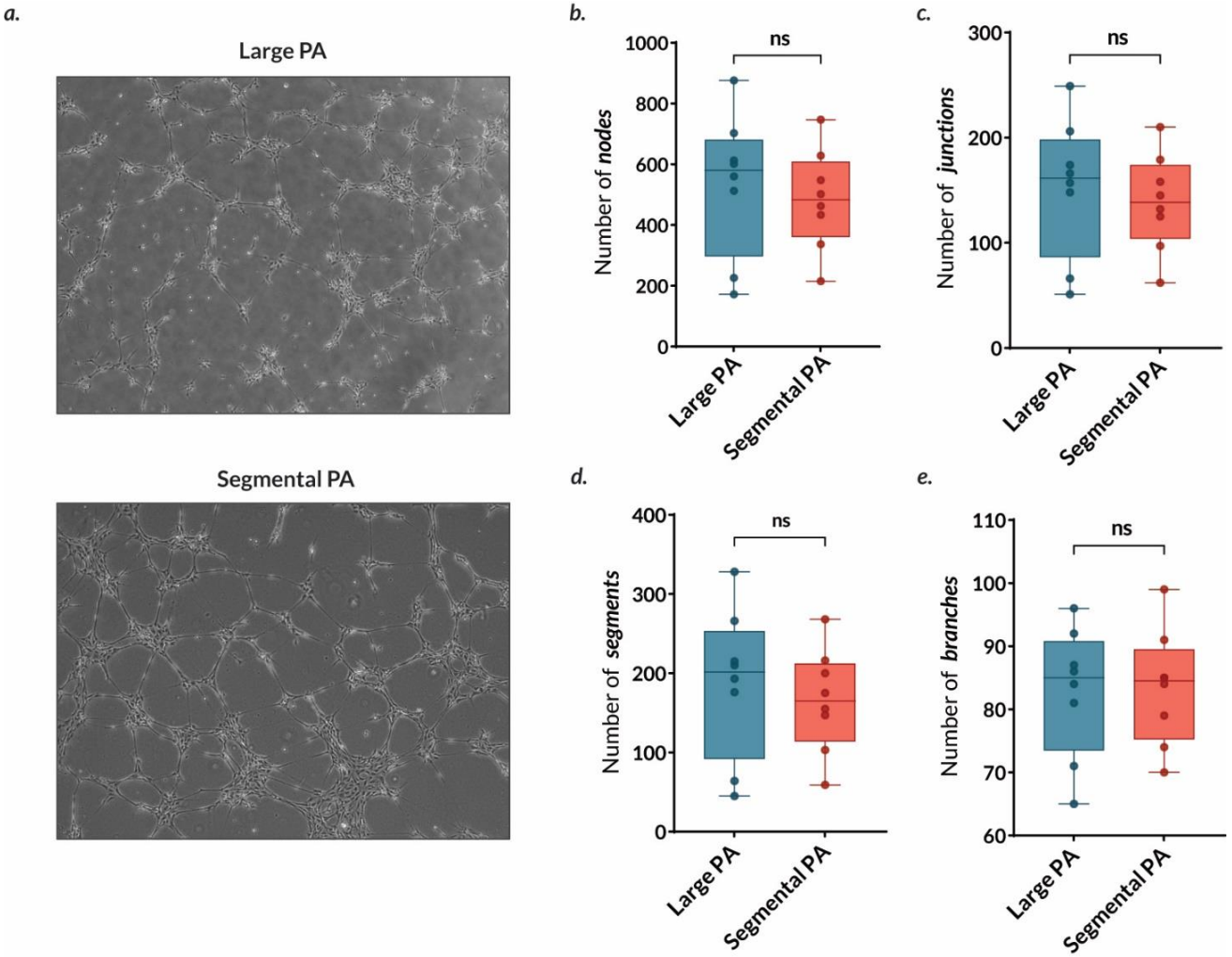

Figure 7: Tube formation capacity of PAECs isolated from large and segmental pulmonary arterial lesions of CTEPH patients. Representative pictures of tube formation capacity of large and segmental PAECs **(a)**. Tube formation capacity was assessed by counting the number of nodes **(b)**, junctions **(c)**, segments **(d)**, and branches **(e)**. Two independent experiments per patient (n=8) were carried out in triplicate between passages 3 and 7 and expressed as median (25^{th}-75^{th} interquartile range). Comparisons by paired Student t-test (**b-e**). ns, non significant; PAECs, pulmonary artery endothelial cells; PA, pulmonary artery.

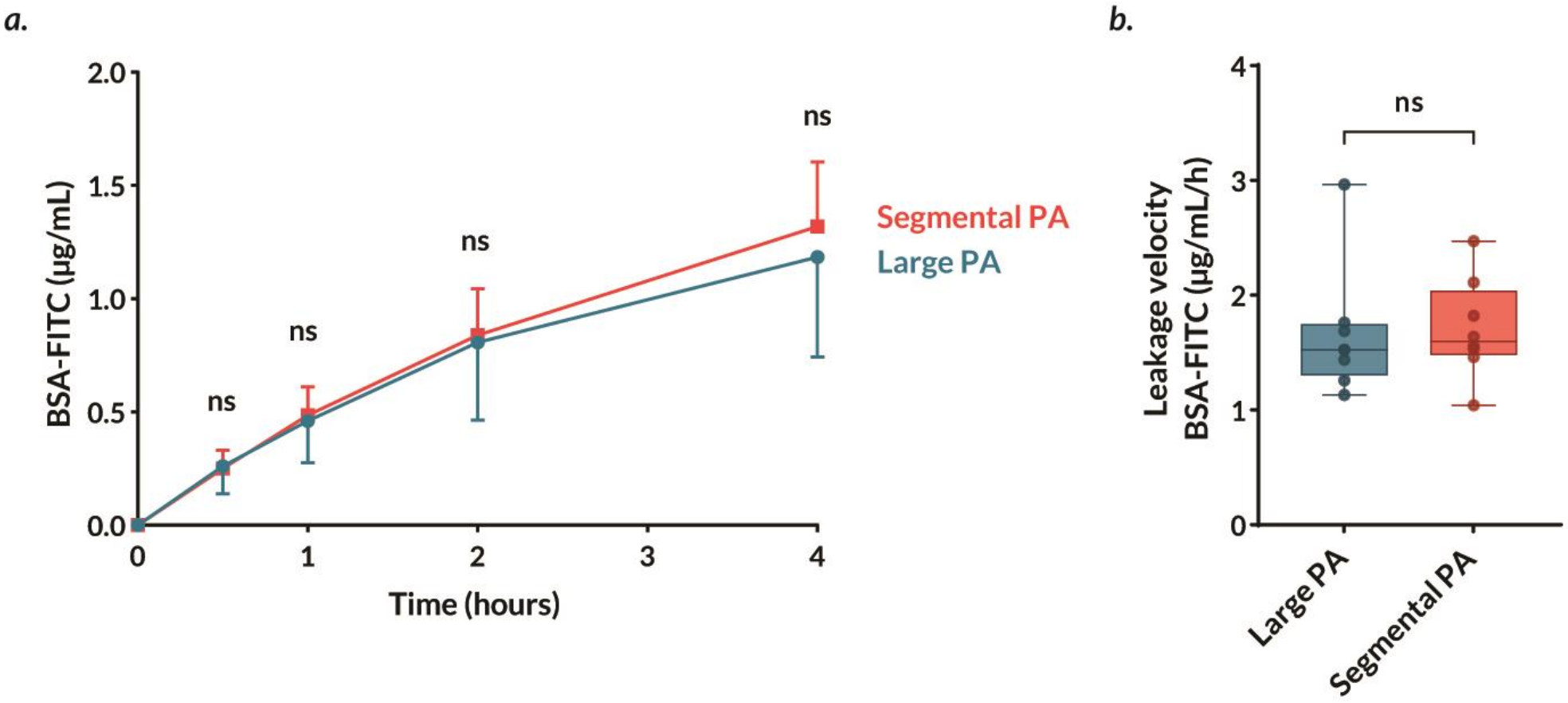

Figure 8: Barrier function of PAECs isolated from large and segmental pulmonary arterial lesions of CTEPH patients. Leakage of BSA-FITC (µg/mL) through large and segmental PAECs monolayer was assessed over time **(a)**. Averaged BSA-FITC leakage velocity (µg/mL/h) through large and segmental PAECs monolayer was evaluated by measuring the area under the curve **(b)**. Two independent experiments per patient (n=8) were carried out in duplicate between passages 3 and 6 and expressed as median (25^{th}-75^{th} interquartile range). Comparisons by two-way ANOVA and post-hoc Šídák's test **(a)** and paired Wilcoxon t-test **(b)**. ns, non significant; PAECs, pulmonary artery endothelial cells; PA, pulmonary artery.